

Subcritical Limits for Plutonium Systems

H. K. Clark

*E. I. du Pont de Nemours & Co.
Savannah River Laboratory
Aiken, SC 29808*

Received December 1, 1980

Accepted April 14, 1981

As a contribution to a required review of American National Standard for Nuclear Criticality Safety in Operations with Fissionable Materials Outside Reactors, limits for plutonium systems have been recalculated to confirm their subcriticality under the stated conditions or to propose other values. Additional limits were calculated for $\text{Pu}(\text{NO}_3)_4$ solutions that allow credit for the presence of ^{240}Pu . Limits were calculated for PuO_2 . Three methods were used to calculate limits for aqueous solutions. Only the two S_n methods were applied to metal and oxide. The validity of each was established by extensive correlation with critical experiments, and in some cases with experiments performed subsequent to the original limit calculations.

I. INTRODUCTION

The procedures of the American National Standards Institute (ANSI) require that action be taken to reaffirm, revise, or withdraw a Standard no later than five years from the date of its publication. Accordingly, a review has been started of American National Standard for Nuclear Criticality Safety in Operations with Fissionable Materials Outside Reactors.¹ As the result of a recommendation² that the dimensional limits for aqueous solutions of ^{235}U be reduced, the independent calculation of all the limits in the Standard was considered to be an important part of this review, and was begun with plutonium systems. In the process, it seemed worthwhile to calculate additional limits to propose for inclusion in the Standard, particularly limits for oxides and various isotopic compositions of plutonium.

Limits in the Standard are intended to be "maximum subcritical limits," i.e., close enough to critical to discourage attempts to derive slightly larger values,

¹"American National Standard for Nuclear Criticality Safety in Operations with Fissionable Materials Outside Reactors," N16.1-1975 (ANS-8.1), American Nuclear Society (1975).

²S. R. McNEANY and J. D. JENKINS, *Nucl. Sci. Eng.*, **65**, 441 (1978).

but actually subcritical under the stated conditions. The stated conditions (infinite systems, absence of neutron absorbing vessel walls, plutonium solutions without free nitric acid, optimum concentrations, etc.) may be ones that are difficult or impossible to create. Furthermore, as the Standard emphasizes, the limits are not intended as operating limits; margins must be allowed to provide for operating contingencies. However, it would be improper to count on these factors and to specify limits in the Standard that are not confidently expected to be subcritical under the stated conditions. It should be legitimate for the user of the Standard (conservatively) to make adjustments in the limits to take advantage of the extent to which credible potential conditions in his operation may deviate from the stated conditions.

II. CALCULATIONAL METHODS

Three one-dimensional calculational methods were selected for this work and require an assumption of separability of the neutron flux into a product of spatial components to be applied to finite cylinders or slabs. Each has its advantages and disadvantages. All three were validated by correlation with critical experiments. All the computer codes included in these methods are modules in the Savannah River

Laboratory JOSHUA system.³ A driver module, KOKO, has been written to prepare standardized input and to execute the codes in specified sequences.⁴ Brief descriptions of the methods are given below; full descriptions are contained in a more extended account of the present work⁵ and in internal memoranda that will be made available to anyone obtaining the JOSHUA system and the computer codes.

The oldest method, designated MGBS-TGAN, comprises the MGBS and TGAN computer codes.⁶ The MGBS code has a 12-group structure. It incorporates the cross sections of Yiftah et al.⁷ collapsed to the group structure of Loewenstein and Okrent⁸ for the top ten groups. The thermal group contains cross sections derived by Amster⁹ with extrapolation provided when $4 < H/^{239}\text{Pu} < 100$. Resonance integrals as a function of potential scattering are provided for the eleventh group. For the top 11 groups, moderator cross sections for nitric acid solutions, for carbon, and for oxygen were derived from infinite medium, multigroup calculations with lethargy width 0.1, and with a ^{235}U fission source. The code performs a B_0 calculation to obtain the critical (unadjusted for bias) buckling. The resulting spectrum is used to collapse cross sections for core materials in the top 11 groups to a set of fast-group cross sections. The removal cross section and neutrons per fission in each of the two resulting groups are then adjusted so as to preserve transport cross sections, absorption cross sections, buckling, and fast-to-slow flux ratio in a diffusion theory formulation. Cross sections for reflector materials are collapsed at zero buckling. Cross sections for vessel walls are collapsed in the reflector spectrum.

The adjusted two-group cross sections are used in the analytical two-group diffusion theory code TGAN to compute either critical transverse buckling (even for spheres) or critical size (with any specified trans-

verse buckling). The effective neutron multiplication factor k_{eff} is computed as

$$k_{\text{eff}} = \frac{1 + M^2 B_c^2}{1 + M^2 (B_c^2 - B_{tr}^2)}, \quad (1)$$

where

B_c^2 = critical buckling computed by MGBS

M^2 = corresponding migration area

B_{tr}^2 = transverse buckling computed by TGAN.

The combination $B_c^2 - B_{tr}^2$ is the geometric buckling. In the case of finite bodies (other than spheres), it consists of two or three terms involving critical transverse bucklings computed for each dimension, i.e.,

$$B_g^2 = \sum_{i=1}^n (B_c^2 - B_{tr,i}^2). \quad (2)$$

A second method (HRXN-ANISN) employs Hansen-Roach¹⁰ cross sections (plus some others with the same group structure), essentially as furnished with KENO IV (Ref. 11), in conjunction with S_n transport theory calculations as performed by the ANISN code.¹² Macroscopic cross sections are prepared by HRXN, which computes potential scattering and corresponding resonance cross sections by three-point Lagrange interpolation in terms of the logarithm of potential scattering per absorber atom. The HRXN code computes atom densities from composition data and performs a B_1 calculation for each mixture. The cross-section set selected for hydrogen is that produced by fission spectrum weighting (Tables XIX and XX of Ref. 10). The plutonium fission spectrum is that given in Table IV of Ref. 10.

Completely symmetric quadrature sets satisfying even moment conditions¹³ are used in the ANISN calculations, which, in correlations to establish bias, were done for orders 4, 8, and 16. Extrapolation to S_∞ is done according to the formula

$$P_\infty = \frac{32P_{16} - 12P_8 + P_4}{21}, \quad (3)$$

³H. C. HONECK, "The JOSHUA System," DP-1380, Savannah River Laboratory (1975).

⁴H. K. CLARK, *Trans. Am. Nucl. Soc.*, **28**, 281 (1978).

⁵H. K. CLARK, "Correlation of Nuclear Criticality Safety Computer Codes with Plutonium Benchmark Experiments and Derivation of Subcritical Limits," DP-1565, Savannah River Laboratory (to be published).

⁶H. K. CLARK, "Computer Codes for Nuclear Criticality Safety Calculations," DP-1121, Savannah River Laboratory (1967).

⁷S. YIFTAH, D. OKRENT, and P. A. MOLDAUER, "Fast Reactor Cross Sections," International Series of Monographs on Nuclear Energy, Division II, Nuclear Physics, Vol. 4, Pergamon Press, Inc., Maxwell House, Elmsford, New York (1960).

⁸W. B. LOEWENSTEIN and D. OKRENT, *Proc. Int. Conf. Peaceful Uses of Atomic Energy*, Geneva, Switzerland, September 1-13, 1958, **12**, 16 (1958).

⁹H. J. AMSTER, "A Compendium of Thermal Neutron Cross Sections Averaged over the Spectra of Wigner and Wilkins," WAPD-185, Bettis Atomic Power Laboratory (1958).

¹⁰G. E. HANSEN and W. H. ROACH, "Six and Sixteen Group Cross Sections for Fast and Intermediate Critical Assemblies," LAMS-2543, Los Alamos National Laboratory (1961).

¹¹L. M. PETRIE and N. P. CROSS, "KENO-IV, An Improved Monte Carlo Criticality Program," ORNL-4938, Oak Ridge National Laboratory (1975).

¹²W. W. ENGLE, Jr., "A User's Manual for ANISN, A One-Dimensional Discrete Ordinates Transport Code with Anisotropic Scattering," K-1693, Oak Ridge Gaseous Diffusion Plant (1967).

¹³K. D. LATHROP and B. G. CARLSON, "Discrete Ordinates Angular Quadrature of the Neutron Transport Equation," LA-3186, Los Alamos National Laboratory (1965).

which is obtained by fitting a third-order polynomial in the reciprocal of the order of quadrature to values of any parameter P_n calculated by S_n with the requirement that the slope be zero when the reciprocal is zero. Mesh is assigned according to the formula¹⁴

$$\Delta R = \frac{1.0 + (\Sigma_g^0 - g/\Sigma_g)}{4\Sigma_g}, \quad (4)$$

where g is the group in which Σ has its maximum value. Generally, this formula results in an excessively large number of intervals, and a scheme is used that is based on several criteria¹⁴ and that assigns a variable mesh that is successively coarser (by a factor of 2) in subzones away from material boundaries. The subzones within a medium all have the same number of intervals, and enough subzones are provided to prevent this number from exceeding ten.

A module SPBL applies ANISN to the determination of k_{eff} of two- or three-dimensional bodies with separability assumed. An ANISN k_{eff} search is performed for each dimension with the other dimensions assumed infinite, i.e., with zero transverse buckling. The two (finite cylinder) or three (cuboid) values of k_{eff} are supplied to SPBL together with the macroscopic cross sections of the core material. For each value of k_{eff} , a B_1 calculation is made to determine the corresponding buckling, which is interpreted as the geometric buckling. These bucklings are combined, and k_{eff} is calculated (again by B_1) for the body. For large bodies, this approach is quite good since geometric bucklings are determined largely by the dimensions. For small bodies, it tends to overestimate k_{eff} . For a series of bodies, in which a dimension is progressively reduced, the transverse buckling is also reduced. Extrapolation to zero transverse buckling then yields k_{eff} for an infinite slab or cylinder.

The third method (GLASS-ANISN) employs largely ENDF/B-IV cross sections (cross sections for carbon, chromium, nickel, and ²⁴¹Am were processed from older libraries) in conjunction with S_n transport theory calculations, again as performed by ANISN. The ANISN calculations are no different from those with Hansen-Roach cross sections. The ENDF/B-IV cross sections were processed into the 84-group structure of GLASS (Ref. 3) [identical with the 84-group structure of HAMMER (Ref. 15): 54 MUFT groups, 30 THERMOS groups]. Resonance parameters are processed into modules that perform the Nordheim resonance calculation for core material and convert

the results into reaction rates per slowing down source for each of the groups containing resonances. A special version of one of the GLASS modules limits scattering to P_0 for the heavier ($A > 27$) nuclides and to P_1 for the lighter nuclides. It implements the extended transport approximation as has been done in the Hansen-Roach¹⁰ cross sections.

Subroutines of KOKO compute atom densities required by GLASS from composition data as in HRXN. Additional subroutines convert the resonance reaction rates to cross sections and formulate 84-group macroscopic cross sections for each material. (The GLASS code eventually converts the reaction rates to cross sections in the process of collapsing to few-group diffusion theory parameters, but for the present purposes it was convenient to use GLASS modules only for formulating smooth 84-group macroscopic cross sections and for calculating resonance reaction rates.) A B_1 calculation in KOKO (that in GLASS is bypassed) computes the critical (unadjusted for bias) buckling for core material and the corresponding flux moments 0, 1, and 2. The moments are used to collapse the 84-group cross sections to a 16-group structure, as close as possible to the Hansen-Roach structure. Transport cross sections are determined from the appropriate ratio of moments so that the critical buckling is preserved. A fission source characteristic of core material accompanies the cross sections. In reflector material, the collapsing is at zero buckling with a ²³⁹Pu fission source. For vessel walls, the cross sections are collapsed with the reflector spectrum. Upscatter is removed in a manner that preserves the flux moments.

The B_1 spectrum developed in core material was not appropriate for weighting cross sections in the lower groups in cases where the core is metal or even damp oxide and the reflector is water or plastic. In these cases (with or without a reflector), only in the first six groups (>15 keV) are the cross sections weighted by flux moments developed in core material at critical buckling. In the remaining ten groups, the cross sections are weighted by the moments developed in a 50-50 mixture (by volume) of core material and water at zero buckling. Transport cross sections in these groups are weighted in a straightforward manner by first-order flux moments.

Where limits calculated by the three methods disagree, one might be inclined to give credence to GLASS-ANISN, which has cross sections derived from ENDF/B-IV including cross sections for hydrogen in the lower groups conforming to a thermal scattering law for water. Moreover, GLASS makes use of resonance parameters by way of the Nordheim integral treatment (although something seems amiss in the resonance treatment since at very high concentrations of fissile nuclides, resonance reaction rates exceed source rates from slowing down) and ANISN makes use of S_n transport theory in 16 groups for

¹⁴R. G. SOLTESZ et al., "Nuclear Rocket Shielding Methods Modification, Updating, and Input Data Preparation. One Dimensional Discrete Ordinates Transport Technique," WANL-PR(LL)-034 (Vol. 4), Westinghouse Astronuclear Laboratory (1970).

¹⁵J. E. SUICH and H. C. HONECK, "The HAMMER System," DP-1064, Savannah River Laboratory (1967).

performing the reactor calculation. However, the older, more approximate method MGBS-TGAN (Ref. 6) cannot be dismissed out of hand as being overly conservative. The GLASS cross sections collapsed to 2 groups rather than 16, adjusted for the difference in leakage expressions between diffusion theory and transport theory, gave close to the same bias in GLASS-TGAN calculations as was obtained in 16-group GLASS-ANISN calculations for ^{235}U solutions, especially at the lower concentrations; hence, two-group diffusion theory is not grossly inadequate. The resonance integrals in MGBS are tabulated as a function of potential scattering cross section per atom of absorber with special care not to include ^{240}Pu contributions below the thermal energy cutoff. The nitrogen, hydrogen, and oxygen cross sections in the epithermal groups are functions of nitrate concentration, and were determined at nitrogen-to-hydrogen atomic ratios of 0, 0.04, and 0.08 in infinite medium, zero buckling calculations with a fission source. The thermal group cross sections have been averaged over 110 groups, rather than 29 as in GLASS, albeit having been calculated with the Wigner-Wilkins gas kernel rather than a thermal scattering law for water.⁹ As will be seen, the bias of GLASS-ANISN is larger than that of MGBS-TGAN, but the latter shows more variation with a hydrogen-to-plutonium atomic ratio.

III. EXPERIMENTAL DATA

The calculational methods are one dimensional, as are the limits. Therefore, in establishing bias, the principal interest is in critical experiments with spheres, and with finite cylinders and cuboids that can readily be extrapolated to infinite cylinders and slabs or that fill in gaps in the data even if separability is assumed in analyzing them. The experiments that were selected are described below with the assumptions that were made in their analysis.

III.A. $\text{Pu}(\text{NO}_3)_4$ Solutions

Many of the limits are for solutions of $\text{Pu}(\text{NO}_3)_4$ and many critical experiments have been performed with such solutions in which free nitric acid, plutonium concentration, plutonium isotopic composition, and vessel size were variables. It is important in analyzing such data and subsequently in calculating limits to have a consistent recipe for computing solution density as a function of plutonium concentration and acid normality. It is desirable that the recipe be fairly accurate if bias derived from correlations with nitrate solutions is to be applied with confidence to oxide-water mixtures, particularly at high concentration. The development of such a recipe is complicated by some lack of consistency in reported analytical data. Nitrate concentrations, plutonium concentrations, and acid normalities are frequently not exactly con-

sistent with a stated valence of 4 for plutonium. The recipe adopted considered solutions of $\text{Pu}(\text{NO}_3)_4$, with varying amounts of HNO_3 , to be solutions of PuO_2 in nitric acid solutions.

The densities of nitric acid solutions as functions of concentration and temperature are well known. The volume apparently displaced by a mole of PuO_2 (the apparent molal volume) in nitric acid solutions may be determined from these densities and plutonium solution composition data. Analysis of composition data reported for $\text{Pu}(\text{NO}_3)_4$ solutions¹⁶⁻¹⁸ in conjunction with nitric acid densities given in International Critical Tables led to much scatter in the apparent molal volume of PuO_2 (particularly at low concentrations), too much to be able to detect any conceivable dependence on free-acid concentration. The following values were, somewhat arbitrarily, selected to correspond, respectively, to plutonium molarities of 0, 0.5, 1.0, 1.5, and ≥ 2.0 : -10.3, 2.7, 7.3, 9.5, and 10.3 cm^3 . These values, along with nitric acid density tables expressed as functions of molarity and temperature, are incorporated in HRXN and in the KOKO subroutines for preparing GLASS input, and five-point Lagrangian interpolation of the apparent molal volumes is provided. The calculation of solution density requires then only the specification of plutonium concentration (and isotopic composition), temperature, and total nitrate concentration. This approach was preferred over density data reported for the critical experiments, with hydrogen density obtained by difference and thereby containing the cumulative error, and to the use of density formulas in view of the lack of agreement among those that have been proposed.

One of the earlier formulas is¹⁹

$$\rho = 1 + 0.031H + 0.00146C,$$

where H is the free acid molarity and C is the plutonium concentration in g/l. Guibergia,²⁰ covering the concentration range 12 to 166 g/l, the acid molarity range 1.51 to 2.16 M , and a temperature range from 20 to 50°C, derived the formula

$$\rho = d + 0.034H + 0.00147C,$$

¹⁶R. C. LLOYD, C. R. RICHEY, E. D. CLAYTON, and D. R. SKEEN, *Nucl. Sci. Eng.*, **25**, 165 (1966).

¹⁷F. BARBRY, J. C. BOULY, R. CAIZERGUES, E. DEILGAT, M. HOUELLE, and P. LECORCHE, "Etude Experimentale et Theorique de l'Empoisonnement Heterogen de Solution de Matiere Fissile par des Tubes ou des Anneaux en Verre au Borosilicate," CEA-R-3931, Commissariat à l'Energie Atomique (1969).

¹⁸R. C. LLOYD, S. R. BIEMAN, and E. D. CLAYTON, *Nucl. Sci. Eng.*, **50**, 127 (1973).

¹⁹*Reactor Handbook*, Vol. II, p. 445, Wiley Interscience Publishers, Inc., New York (1961).

²⁰J. G. GUIBERGIA, "Densité des Solutions Nitriques de Plutonium," CEA-1698, Commissariat à l'Energie Atomique (1960).

where d is the density of water at the appropriate temperature. From a least-squares analysis of the density of a large number of $\text{Pu}(\text{NO}_3)_4$ solutions, Richey²¹ derived the following expression for the concentration of water:

$$\text{H}_2\text{O} (\text{g}/\ell) = 1000 - 0.3619 \text{ g Pu}/\ell - 24.6H$$

Richey²² later corrected the coefficient of acid molarity to 33.1. From the corrected expression, the formula derived for the density of $\text{Pu}(\text{NO}_3)_4$ solutions is

$$\rho = 1 + 0.0299H + 0.001675C$$

Before correction, the acid molarity coefficient was 0.0384. The acid molarity coefficient is suspect, however. For aqueous solutions of nitric acid, the coefficient at 20°C is 0.0338 as determined by densities at 0 and 0.81 M and 0.0314 as determined by densities at 0 and 7.9 M , but the density is obviously not strictly a linear function of molarity. For a solution containing 160 g Pu/ℓ , 2.2 M acid, the densities obtained from Richey's corrected formula and from the French formula differ by $\sim 2\%$; the corresponding difference in k_{eff} calculated for a nearly critical water-reflected sphere is ~ 0.01 .

The P-11 project includes a large number of critical experiments done with $\text{Pu}(\text{NO}_3)_4$ solutions contained within thin spherical shells of stainless steel and two within a shell of aluminum.²³ Nominal diameters for water-reflected spheres were 11, 12, 13, 14, and 15 in., and a bare sphere was 16 in. in diameter. In these experiments, the reported critical masses are not exactly the product of the reactor volume and the concentration, due presumably to a correction made for the control rod and perhaps for the sphere neck. In the listing of the experimental data in Table I, the plutonium concentrations are the quotients of the reported critical masses and the sphere volumes. In this and subsequent tables, the plutonium isotopic composition is given in weight percent of isotopes other than ²³⁹Pu. Radii are calculated from volumes. Where experiments appeared to be duplicate runs, averages were taken. The reported experimental uncertainties are small. The critical masses are estimated to be within $\pm 1.5\%$, the sphere volumes within $\pm 0.3\%$, the nitrate ion concentrations within $\pm 0.6\%$, and the percentages of ²⁴⁰Pu within $\pm 7\%$. Densities calculated from nitric acid tables and the apparent molal volumes of PuO_2 were generally less than the reported values. The maximum underestimation was 1.27%, the next largest, 0.82%, and the maximum overestimation, 0.31%. On the average, the density was underestimated by 0.20%.

The P-11 project also includes experiments with water-reflected cylinders, and, although separability must be assumed in analyzing the experiments by one-dimensional methods, some correlations were made to establish the validity of applying bias determined with spheres to calculations for infinite cylinders. Temperature was slightly more variable than in the sphere experiments, but variations were not taken into account in the correlations. Many of the nitrate concentrations were estimates, due perhaps to an initial failure to recognize its significant bearing on critical mass. The cylinders were reflected on all surfaces. The critical conditions are given in Table II. The discrepancy between calculated and reported densities was larger for these experiments, with more scatter, ranging from an underestimation of 1.55% to an overestimation of 0.83% and averaging out to an underestimation of 0.45%.

Results of a second series of critical experiments with spheres of $\text{Pu}(\text{NO}_3)_4$ solution, begun at the Critical Mass Laboratory at Hanford, Washington, in 1961, were published by Lloyd et al.¹⁶ An analysis of these experiments and the P-11 project experiments was published by Richey,²¹ and contained some data not in the earlier publication. The conditions for the experiments selected are listed in Table III. The sphere radii, derived from volumes, have been modified to take account of an empirically determined correction for the vessel neck. For the 14 experiments reported by Lloyd et al. (Richey reported no densities), calculated densities again generally underestimated reported densities ranging from an underestimation of 1.03% to an overestimation of 0.21% and averaging out to an underestimation of 0.38%. An analysis of the experimental error by Lloyd et al. led to an estimate of an uncertainty of about $\pm 1\%$ in the critical mass except for the two experiments where $\text{Pu}(\text{VI})$ and polymer were present, and where the uncertainty was estimated to be $\pm 5\%$.

The only other experiment with spheres was a recent one²⁵ utilizing the large sphere of Gwin and Magnuson²⁶ to better establish the minimum critical concentration of ²³⁹Pu. In Ref. 25, solution analyses from two different laboratories were presented, differing by $\sim 1.5\%$. Recently, however, the higher of the two sets has been discarded,²⁷ since it was of poorer quality. No nitrate concentration was reported; it was inferred from the valency of $\text{Pu}(\text{IV})$ and from the

²⁴B. M. DURST, S. R. BIERMAN, and E. D. CLAYTON, "Handbook of Critical Experiments Benchmarks," PNL-2700, Pacific Northwest Laboratory (1978).

²⁵R. C. LLOYD, R. A. LIBBY, and E. D. CLAYTON, *Trans. Am. Nucl. Soc.*, **28**, 292 (1978).

²⁶R. GWIN and D. W. MAGNUSON, *Nucl. Sci. Eng.*, **12**, 364 (1962).

²⁷R. C. LLOYD, Battelle-Pacific Northwest Laboratories, Private Communication (1980).

²¹C. R. RICHEY, *Nucl. Sci. Eng.*, **31**, 32 (1968).

²²C. R. RICHEY, *Nucl. Sci. Eng.*, **49**, 246 (1972).

²³F. E. KRUESI, J. O. ERKMAN, and D. D. LANNING, "Critical Mass Studies of Plutonium Solutions," HW-24514, Hanford Atomic Products Operation (1952).

TABLE I
Critical Spheres of Pu(NO₃)₄ Solution
(P-11 Project, Ref. 23)

Chemical Composition			²⁴⁰ Pu (wt%)	Temperature (°C)	Radius (cm)	Chemical Composition			²⁴⁰ Pu (wt%)	Temperature (°C)	Radius (cm)
g Pu/ℓ	g NO ₃ /ℓ	g Fe/ℓ ^a				g Pu/ℓ	g NO ₃ /ℓ	g Fe/ℓ ^a			
Water Reflector ^b						Water Reflector ^b					
135.8 ^c	229.0	0.464	3.12	27	13.95 ^d	29.72	111.3	0.123	3.12	27	17.80
50.16	138.5	0.189	3.12	27	15.36	30.16	143.0	0.113	3.12	27	17.80
51.74	163.0	0.272	3.12	27	15.36	31.81	208.0	0.120	3.12	27	17.80
56.42	207.0	0.245	3.12	27	15.36	35.55	309.5	0.145	3.12	27	17.80
59.97	237.0	0.192	3.12	27	15.36	39.55	408.0	0.147	3.12	27	17.80
63.66	270.0	0.197	3.12	27	15.36	29.86	87.5	0.128	4.05	27	17.80
70.44	322.0	0.218	3.12	27	15.36	30.73	119.3	0.079	4.05	27	17.80
77.42	359.0	0.237	3.12	27	15.36	31.64	146.8	0.086	4.05	27	17.80
36.25	93.1	0.114	3.12	27	16.27 ^e	33.76	210.7	0.097	4.05	27	17.80
37.08	125.0	0.128	3.12	27	16.27	36.25	272.4	0.104	4.05	27	17.80
33.55	86.7	0.124	1.76	27	16.54	38.71	335.2	0.126	4.05	27	17.80
34.58	116.5	0.177	1.76	27	16.54	41.12	384.9	0.126	4.05	27	17.80
35.37	145.0	0.124	1.76	27	16.54	30.80	126.5	0.108	4.40	27	17.80
37.70	130.0	0.103	3.12	27	16.54	32.06	158.0	0.102	4.40	27	17.80
38.38	156.0	0.141	3.12	25	16.54	24.97	116.0	0.088	3.12	27	19.06
40.92	205.0	0.257	3.12	27	16.54	25.73	147.0	0.094	3.12	27	19.06
44.35	269.5	0.266	3.12	27	16.54	27.15	212.0	0.096	3.12	27	19.06
26.48	77.8	0.145	0.54	27	17.80	Unreflected					
26.50	107.0	0.149	0.54	27	17.80						
27.39	137.5	0.156	0.54	27	17.80	35.59	106.9	0.112	4.15	23	20.13
28.28	187.5	0.164	0.54	27	17.80	38.13	163.0	0.124	4.15	24	20.13
27.77	109.5	0.094	1.76	27	17.80	38.16	180.0	0.178	4.15	23	20.13
28.81	87.4	0.110	3.12	27	17.80	43.43	281.8	0.179	4.15	22	20.13

^aThe iron was assumed present as Fe₂O₃ with a 5.24 g/cm³ density.

^bWater thickness was ≥12 in.

^cThis solution was subcritical by an unknown amount.

^dExcept where noted to the contrary, the solution was enclosed by a Type 347 stainless steel shell. The composition assumed was 70% iron, 18% chromium, 12% nickel with an 8.0 g/cm³ density. The thickness was 0.05 in. (0.127 cm).

^eThe solution was enclosed by an aluminum shell. The density was assumed to be 2.7 g/cm³. The thickness was 20 gauge (0.081 cm).

reported HNO₃ molarity. The critical concentration was interpolated from extrapolations to critical volumes that bracketed the actual volume of the sphere. Table IV gives the critical conditions as determined by the two sets of measurements. The critical plutonium concentrations were determined from a power fit to the data. Linear interpolations of the concentrations for the critical volumes on either side of the actual volume appear equally valid and lead to 9.618 and 9.457 g Pu/ℓ for the two sets of measurements. The acid molarities are linear interpolations. Densities calculated from apparent PuO₂ molal volumes and nitric acid tables underestimate the reported densities by 0.11 and 0.22%, but den-

sities calculated from reported atom densities underestimate the reported solution densities by 0.25 and 0.40%.

A series of experiments has been done in a slab tank of adjustable thickness, both bare and reflected by water.²⁸ Plutonium containing ~5% ²⁴⁰Pu and ~20% ²⁴⁰Pu was used. The data have been extrapolated to completely bare infinite slabs and to infinite, water-reflected slabs with no intervening wall. The extrapolated critical conditions are listed in Table V. Sizable corrections were required for tank

²⁸R. C. LLOYD, E. D. CLAYTON, L. E. HANSEN, and S. R. BIERMAN, *Nucl. Technol.*, **18**, 225 (1973).

TABLE II
Critical Water-Reflected Cylinders of Pu(NO₃)₄ Solution*
(P-11 Project, Ref. 23)

²⁴⁰ Pu (wt%)	Chemical Composition			Height (cm)
	g Pu/ℓ	g NO ₃ ⁻ /ℓ	g Fe/ℓ	
Radius 10.16 cm				
2.85	77.40	152.0	0.644	48.29 ^a
Radius 11.43 cm				
2.83	109.16	166.0	0.395	29.87
2.83	99.09	136.5	0.378	30.71
2.83	85.14	151.0	0.321	32.33
2.83	73.92	125.6	0.231	35.41
2.83	61.49	134.0	0.303	40.08
2.83	54.33	119.8	0.257	44.58
Radius 12.70 cm				
2.85	77.40	152.0	0.644	25.22
2.85	76.93	152.0	0.327	24.74
2.85	62.47	146.0	0.269	27.25
2.85	49.26	142.0	0.260	32.69
2.85	39.10	138.0	0.172	41.76
Radius 13.97 cm				
2.90	63.99	121.1	0.298	22.81
2.90	48.98	139.0	0.238	25.96
2.83	47.21	117.0	0.275	27.08
2.83	41.73	215.0	0.255	32.64
2.85	39.10	138.0	0.172	31.19
2.83	36.90	300.0	0.263	43.00
2.85	33.54	137.0	0.193	39.55
2.85	30.81	136.0	0.173	47.12 ^b
Radius 15.24 cm				
2.83	109.16	166.0	0.395	17.32 ^b
2.90	48.75	116.3	0.223	22.35
2.90	42.29	126.6	0.174	25.25
2.90	36.52	107.1	0.161	28.47
2.90	31.14	114.0	0.153	33.43
2.90	26.45	134.0	0.154	44.45

*The solution temperature was 27°C. The solution was enclosed by stainless steel, with the composition of Table I, 0.062 in. (0.16 cm) thick.

^aSubcritical by an unknown amount.

^b"A reliable extrapolation to the critical height was made." The experiment was subcritical.

walls and support structure and, for the bare slabs, room return. Extrapolation to infinite slab thickness was based on buckling conversions made from bucklings and extrapolation distances determined from several pairs of thickness and critical height measure-

TABLE III
Critical Spheres of Pu(NO₃)₄ Solution*
[Battelle-Pacific Northwest Laboratories (BNPL), Refs. 16,21]

Chemical Composition	
g Pu/ℓ ^a	g NO ₃ ⁻ /ℓ
Water Reflector; Radius 14.55 cm; 0.125-cm-thick Stainless Steel Wall ^b	
73.0	86
74.5	105
96.0	203
100.0	230
119.0	245
126.0	262
132.0	281
140.0	284
269.0	346
295.0 ^c	303
435.0 ^c	372
Radius 17.67 cm; 0.112-cm-thick Stainless Steel Wall	
33.0	162
33.2	164
38.4	292
38.6	292
39.2	313
47.5	462
47.9	465
Radius 19.29 cm; 0.122-cm-thick Stainless Steel Wall	
24.4	58
38.7	517
Unreflected; Radius 19.45 cm; 0.122-cm-thick Stainless Steel Wall	
39.0	64
172.3	486

*The solution temperature was 25°C.

^aThe plutonium contained 4.57% ²⁴⁰Pu, 0.31% ²⁴¹Pu by weight (Ref. 24).

^bThe stainless steel was assumed to have the same composition as in Table I.

^cContained Pu(VI) and polymer.

ments for each composition. The experimenters estimate an uncertainty of ±0.2 cm in the infinite slab thicknesses. Although not as precise as the sphere experiments, the slab experiments are useful in indicating whether bias determined with spheres is appropriate for slabs and in indicating the effect of large isotopic concentrations of ²⁴⁰Pu on the bias. Although solution densities are not given in the final report of the experiments,²⁸ they appear in various

TABLE IV
Critical Bare Sphere of Low Concentration
Plutonium Solution*

Chemical Composition		Aluminum Wall (cm)	Radius (cm)
g Pu/ℓ ^a	g NO ₃ /ℓ		
9.598 ^b	68.801	0.77	61.00
9.426	78.294	0.77	61.00

*The solution temperature was 23°C.

^aThe plutonium contained 0.004% ²³⁸Pu, 2.521% ²⁴⁰Pu, 0.075% ²⁴¹Pu, 0.014% ²⁴²Pu by weight.

^bOmitted from later report as being less reliable.

BNL reports²⁹ issued during the course of the experiments. Calculated densities, with ²⁴¹Am assumed present as AmO₂ with a density of 11.6 g/cm³, agreed well with reported densities, ranging from an underestimation of 0.02% to an overestimation of 0.52%.

Some experiments in cylinders, water reflected on sides and bottom, bare on top, have been done^{24,30} with plutonium containing ~43% ²⁴⁰Pu. These experiments are useful for indicating the bias to be used in calculating limits for systems with high ²⁴⁰Pu concentrations, although the assumption of separability introduces some uncertainty. Some gadolinium was

²⁹See, for example, R. C. LLOYD, S. R. BIERMAN, C. A. ROGERS, and R. D. JOHNSON, "Reactor Physics Quarterly Report January, February, March 1969," BNL-1053, p. 5.6, Battelle-Pacific Northwest Laboratories (1969).

³⁰R. C. LLOYD and E. D. CLAYTON, *Nucl. Sci. Eng.*, **52**, 73 (1973).

present in these experiments, persisting from previous experiments. The critical conditions are given in Table VI.

III.B. Plutonium Oxide

A group of experiments was done with blocks made of essentially dry PuO₂ (H/Pu = 0.04) (Ref. 31). The ²⁴⁰Pu concentration in the plutonium was 18.35%. Temperature variations of as much as 30°C were a problem in performing the experiments; count rates were corrected to 50°C. There was insufficient fuel to make a bare assembly critical, but two bare assemblies were built with driver regions of H/Pu = 5 material so that extrapolation to the bare critical assembly was possible. Its dimensions, corrected empirically for cladding materials and stacking voids, were 30.78 × 30.78 × 20.99 (±0.22) cm. A calculated bare extrapolation distance together with these dimensions yielded a buckling. The thickness reported for the infinite bare slab was derived from the buckling and from a calculated extrapolation distance slightly larger than that calculated for the bare cuboid. The reflected assembly dimensions, corrected for voids, cladding, and temperature effects, are given in Table VII along with composition data (reported only as atom densities) and infinite slab thicknesses.

III.C. Plutonium Metal

Three experiments with plutonium metal spheres were selected: two bare spheres of delta-phase plutonium differing in the isotopic concentrations of ²⁴⁰Pu

³¹S. R. BIERMAN and E. D. CLAYTON, *Nucl. Technol.*, **11**, 185 (1971).

TABLE V
Critical Infinite Slabs*

Chemical Composition		Isotopic Composition (wt%)				Infinite Slab Thickness (cm)	
g Pu/ℓ	g NO ₃ /ℓ	²³⁸ Pu	²⁴⁰ Pu	²⁴¹ Pu	²⁴² Pu	Bare	H ₂ O Reflected
58	203	0.006	4.671	0.255	0.009	16.91	9.13
58	397	0.006	4.671	0.255	0.009	17.99	9.78
66.5 ^a	219	0.19	18.400	4.53	0.96	19.79	11.38
160 ^a	360	0.19	18.400	4.53	0.96	20.05	11.21
241 ^a	495	0.19	18.400	4.53	0.96	21.48	11.64
412 ^a	664	0.19	18.400	4.53	0.96	---	13.01
202 ^b	313	0.07	23.185	3.958	0.966	21.19	11.70
284 ^b	436	0.07	23.185	3.958	0.966	---	12.43

*The temperature was 23°C.

^aThe ²⁴¹Am/Pu weight ratio is 0.0028. Americium was assumed present as AmO₂ with a 11.6 g/cm³ density. Where no cross sections were available for ²⁴¹Am (MGBS and HRXN), it was mocked up by boron with 0.0492 g boron assumed equivalent to 1 g ²⁴¹Am. Boron was assumed present with a 10⁶ g/cm³ density.

^bThe ²⁴¹Am/Pu weight ratio is 0.0021.

TABLE VI

Critical Cylinders of Solution of "High-Burnup" Plutonium*

Chemical Composition		Height (cm)
g Pu/l	g NO ₃ ⁻ /l	
140.0	457.6	54.70
116.0	378.0	50.55
99.3	331.4	48.26
85.5	282.8	47.00
75.6	248.9	47.29
65.1	217.5	49.12
56.3	186.0	52.83
46.8	154.3	63.47
40.6	133.0	80.92

*The temperature was assumed to be 23°C. Inside radius was 30.514 cm. Cylinder walls were stainless steel 0.079 cm thick with composition assumed the same as in Table I; the bottom was 0.95 cm thick (Ref. 24). Cylinders were water reflected on both sides and bottom. The reflector extended to the top of the vessel, which had a 0.95-cm-thick cover. The inside height was ~105 cm (there are small discrepancies in the references). The plutonium contained 0.2% ²³⁸Pu, 42.9% ²⁴⁰Pu, 10.8% ²⁴¹Pu, 4.7% ²⁴²Pu by weight. Americium-241 and gadolinium were present at 1.08 and 0.0089%, respectively, of plutonium concentration. Americium was assumed present as AmO₂ with a 11.6 g/cm³ density, gadolinium as Gd₂O₃ with a 7.407 g/cm³ density. Where no ²⁴¹Am cross sections were available, ²⁴¹Am was mocked up by boron as in Table V. With some inconsistency, boron was assumed present as B₂O₃ with its apparent density of 2.17 g/cm³ in boric acid.

and a water-reflected sphere of alpha-phase plutonium.^{32,33} The critical conditions are given in Table VIII. Radii were derived from reported masses and densities.

IV. CORRELATIONS

Correlations to establish bias were made between the experimental data and the three calculational methods; however, not all methods were applied to all data. The first two methods (MGBS-TGAN and HRXN-ANISN) have previously been applied to some of these data^{6,34}; present correlations differ slightly due to differences in treatment of the data (e.g., the use of apparent molal volumes of PuO₂), the

³²G. E. HANSEN and H. C. PAXTON, "Re-Evaluated Critical Specifications of Some Los Alamos Fast-Neutron Systems," LA-4208, Los Alamos National Laboratory (1969).

³³D. R. SMITH and W. U. GEER, *Nucl. Appl. Technol.*, **7**, 405 (1969).

³⁴E. D. CLAYTON et al., *Nucl. Technol.*, **35**, 97 (1977).

TABLE VII

PuO₂ Compacts

Composition (atom/b·cm)		
²³⁸ Pu		3.383 × 10 ⁻⁵
²³⁹ Pu		1.092 × 10 ⁻²
²⁴⁰ Pu		2.654 × 10 ⁻³
²⁴¹ Pu		7.269 × 10 ⁻⁴
²⁴² Pu		1.632 × 10 ⁻⁴
Oxygen		3.094 × 10 ⁻²
Hydrogen		5.511 × 10 ⁻⁴
Plutonium density (g/cm ³)		5.762
Critical Reflected ^a Array Dimensions (cm)		
L	W	H
25.65	25.65	10.03 ± 0.01
25.65	30.78	8.98 ± 0.01
30.78	30.78	7.97 ± 0.03
30.78	41.05	6.86 ± 0.08
41.05	41.05	5.95
Critical Infinite Slab Thickness (cm)		
Bare		12.17 ± 0.28
Reflected ^a		3.01 ± 0.44 ^b
		3.34 ± 0.10 ^c

^aPlexiglas. Density 1.185 g/cm³; 60% carbon, 32% oxygen, 8% hydrogen by weight, with a thickness of 15 cm (Ref. 24).

^bFrom linear extrapolation of extrapolation distance as a function of inverse cross-sectional area. Plotting against transverse buckling extrapolates to a greater extrapolation distance and reduces the thickness to 2.85 cm.

^cFrom linear extrapolation of thickness as a function of inverse cross-sectional area.

TABLE VIII

Plutonium Metal Spheres

Reflector	Isotopic Composition (at.%)			Radius (cm)	Density (g/cm ³)
	²⁴⁰ Pu	²⁴¹ Pu	²⁴² Pu		
None	4.5	0.3	---	6.385 ± 0.013	15.61 ^a
None	20.1	3.1	0.4	6.660 ± 0.017	15.73 ^b
Water ^c	5.18	0.3	0.02	4.122 ± 0.006	19.74

^aContained 1.02% gallium by weight.

^bContained 1.01% gallium by weight.

^cEffectively infinite. Temperature was assumed to be 20°C.

previous assumption of a temperature of 20°C, and small differences in cross sections. The correlations are expressed as the value of k_{eff} calculated for critical assemblies. The bias is then $(k_{\text{eff}} - 1)$. The uncertainties in the bias corresponding to experimental uncertainties were largely evaluated with HRXN-ANISN.

IV.A. $\text{Pu}(\text{NO}_3)_4$ Solution Spheres

Correlations of HRXN-ANISN, GLASS-ANISN, and MGBS-TGAN with the experiments of Tables I, III, and IV are given in Table IX. The hydrogen-to-fissile-plutonium atomic ratios are those calculated by HRXN and KOKO and differ slightly from those reported by the experimenters. The correlations are listed in the same order as the experiments and are identified by concentration. In the case of GLASS-ANISN, correlations were made with representative experiments rather than the entire set. Apparent densities of PuO_2 , required by MGBS, were obtained from HRXN. The MGBS code assumes a temperature of 20°C; no reduction in density to that at the experimental temperature was made by introducing voids. Consequently, $\text{H}/^{239}\text{Pu}$ ratios calculated by MGBS were slightly higher than those calculated by HRXN. In the MGBS-TGAN calculations for the P-11 experiments, the small amount of iron present was ignored since it was shown to have little effect.

The critical values of k_{eff} from Table IX are plotted against the hydrogen-to-fissile-plutonium atomic ratio in Fig. 1 for HRXN-ANISN, in Fig. 2 for GLASS-ANISN, and in Fig. 3 for MGBS-TGAN. Because of the large influence of this ratio on the neutron spectrum, it was considered to be an impor-

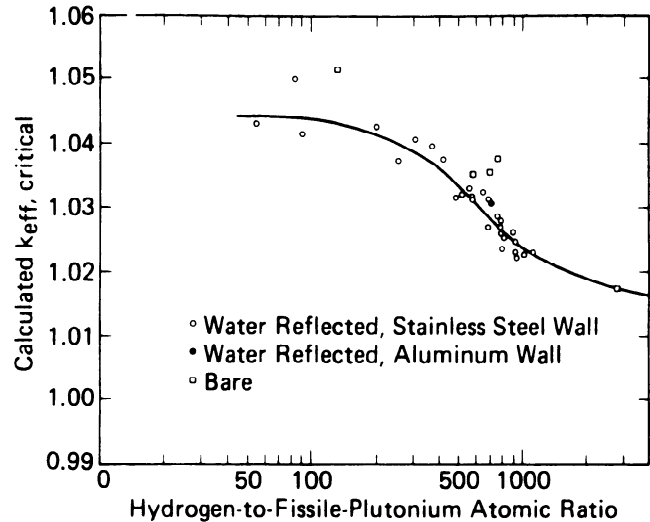


Fig. 2. Values of k_{eff} of experimental critical $\text{Pu}(\text{NO}_3)_4$ solution spheres calculated by GLASS-ANISN (S_{∞}). The line is an "eyeball" fit.

tant parameter, but not necessarily the only one of which bias is a function. However, inspection of the correlations revealed no pronounced trend as a function of nitrate concentration or of ^{240}Pu isotopic concentration. The curves are "eyeball" fits to the data and are drawn through the more reliable point for the large sphere.

Scatter about the curves provides an indication of the uncertainty in the bias. However, the effect on k_{eff} of reported experimental uncertainties was investigated with HRXN-ANISN. In the P-11 project

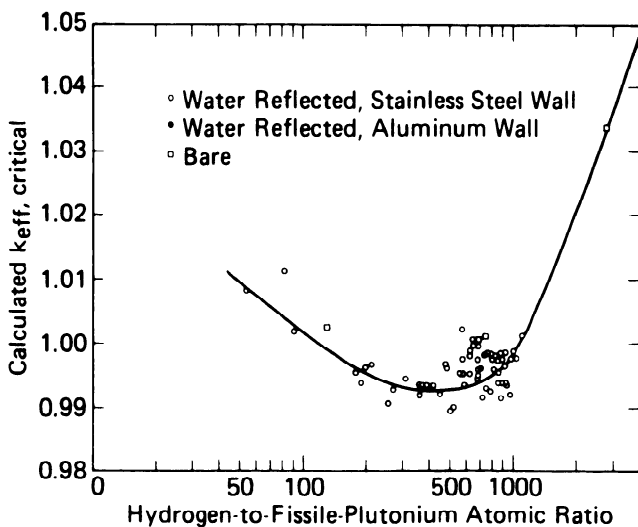


Fig. 1. Values of k_{eff} of experimental critical $\text{Pu}(\text{NO}_3)_4$ solution spheres calculated by HRXN-ANISN (S_{∞}). The line is an "eyeball" fit.

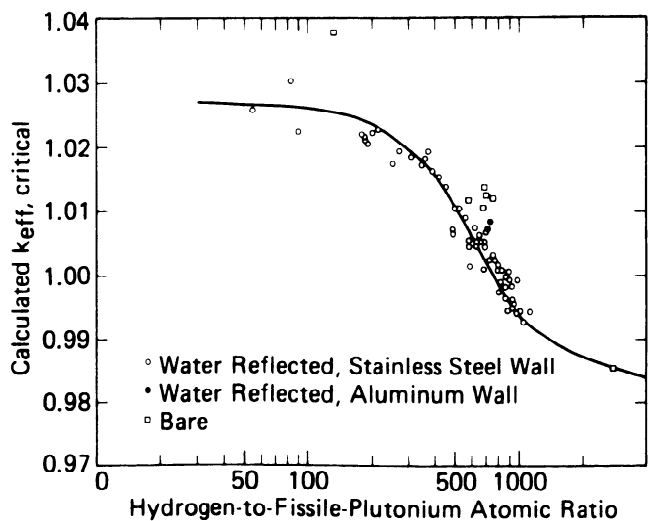


Fig. 3. Values of k_{eff} of experimental critical $\text{Pu}(\text{NO}_3)_4$ solution spheres calculated by MGBS-TGAN. The line is an "eyeball" fit.

TABLE IX

Calculated Values of k_{eff} of the Experimental Critical Spheres of $\text{Pu}(\text{NO}_3)_4$ Listed in Tables I, III, and IV

Plutonium Concentration		k_{eff}		
g Pu/l	H/ $^{239}\text{Pu}^a$	HRXN-ANISN (S_{∞})	GLASS-ANISN (S_{∞})	MGBS-TGAN
135.8	184.5	>0.9906	>1.0398	>1.0213
50.16	518.8	0.9899	1.0320	1.0107
51.74	498.3	0.9894	---	1.0106
56.42	449.4	0.9919	---	1.0139
59.97	417.7	0.9933	1.0375	1.0157
63.66	388.2	0.9933	---	1.0164
70.44	343.2	0.9933	---	1.0172
77.42	307.2	0.9944	1.0406	1.0187
36.25	729.7	0.9981	---	1.0086
37.08	705.3	0.9961	1.0305	1.0071
33.55	779.3	0.9924	1.0268	1.0028
34.58	748.1	0.9926	---	1.0034
35.37	723.8	0.9915	---	1.0027
37.70	692.4	0.9958	1.0311	1.0069
38.38	674.3	0.9943	---	1.0055
40.92	620.2	0.9951	---	1.0077
44.35	557.5	0.9952	1.0330	1.0091
26.48	978.3	0.9976	---	0.9992
26.50	967.4	0.9919	---	0.9940
27.39	925.7	0.9938	1.0229	0.9962
28.28	880.1	0.9914	---	0.9945
27.77	933.8	0.9935	1.0221	0.9958
28.81	920.0	0.9963	1.0247	0.9984
29.72	884.2	0.9985	---	1.0008
30.16	861.4	0.9954	---	0.9983
31.81	796.9	0.9937	1.0235	0.9977
35.55	684.0	0.9950	---	1.0011
39.55	588.5	0.9933	1.0268	1.0017
29.86	896.3	0.9975	1.0258	0.9996
30.73	861.0	0.9973	---	0.9999
31.64	827.9	0.9980	---	1.0010
33.76	757.3	0.9983	1.0285	1.0024
36.25	688.0	0.9994	---	1.0047
38.71	627.3	0.9981	---	1.0049
41.12	577.6	0.9977	1.0311	1.0057
30.80	860.0	0.9938	---	0.9966
32.06	816.6	0.9959	1.0250	0.9991
24.97	1051	0.9975	---	0.9928
25.73	1008	0.9987	1.0225	0.9944
27.15	932.1	0.9985	---	0.9952
35.59	748.7	1.0010	1.0376	1.0121
38.13	684.6	1.0006	---	1.0138
38.16	680.0	0.9974	---	1.0106
43.43	574.3	0.9951	1.0351	1.0118
73	368.9	0.9933	1.0395	1.0196

See footnote at the end of the table.

(Continued)

TABLE IX (Continued)

Plutonium Concentration		k_{eff}		
g Pu/l	H/ ²³⁹ Pu ^a	HRXN-ANISN (S_{∞})	GLASS-ANISN (S_{∞})	MGBS-TGAN
74.5	359.1	0.9917	---	1.0183
96	268.5	0.9929	---	1.0197
100	255.0	0.9905	1.0372	1.0175
119	212.8	0.9967	---	1.0229
126	199.6	0.9961	1.0425	1.0222
132	189.0	0.9945	---	1.0207
140	177.9	0.9961	---	1.0220
269	89.5	1.0018	1.0416	1.0232
295	83.0	1.0113	1.0500	1.0308
435	54.1	1.0081	1.0430	1.0264
33	794.4	0.9974	---	1.0010
33.2	789.1	0.9982	1.0278	1.0018
38.4	648.7	0.9996	---	1.0056
38.6	645.2	1.0005	1.0324	1.0065
39.2	629.7	0.9988	---	1.0053
47.5	485.1	0.9962	1.0316	1.0066
47.9	480.3	0.9967	---	1.0072
24.4	1115	1.0010	1.0230	0.9943
38.7	577.9	1.0022	1.0316	1.0048
39	696.2	0.9960	1.0355	1.0127
172.3	131.3	1.0028	1.0514	1.0380
9.598	2766	1.0440	1.0283	0.9961
9.426	2807	1.0334	1.0174	0.9856

^aIncludes ²⁴¹Pu where specified; hence actually hydrogen-to-fissile-plutonium atomic ratio.

experiments, the uncertainty in the nitrate ion concentration was reported to be within $\pm 0.6\%$, the ²⁴⁰Pu content within $\pm 7\%$, the sphere volume within $\pm 0.3\%$, and the critical mass within $\pm 1.5\%$. The corresponding variations in k_{eff} were evaluated for representative experiments and found to range, respectively, from ± 0.0001 to ± 0.0005 , ± 0.0003 to ± 0.0022 , ± 0.0006 to ± 0.0015 , and ± 0.0013 to ± 0.0039 . The effect on k_{eff} was greatest for the highest nitrate and ²⁴⁰Pu concentrations, the bare sphere, and the lowest plutonium concentrations. Omitting the iron in solution from the P-11 project experiments increases k_{eff} by only ~ 0.0001 . Changing the composition of the steel shell to 2% manganese, 1% silicon, 11% nickel, 18% chromium, and 68% iron reduced k_{eff} by 0.0006 for the reflected spheres and increased it by 0.0001 for the bare spheres. The mass error in more recent experiments¹⁶ was reported to be $\pm 1\%$ except for the two high-concentration solutions, with polymer and Pu(VI) present, where it was $\pm 5\%$. The corresponding variations in k_{eff} ranged, respectively, from ± 0.0003 to ± 0.0020 and from ± 0.0009 to ± 0.0015 . For the 61-cm-radius sphere (Table IV), linear interpolation rather than a power fit to the concentration as a func-

tion of critical volume increased k_{eff} by 0.0014. For this sphere an arbitrary 15% increase in nitrate concentration reduced k_{eff} by 0.0023.

IV.B. Pu(NO₃)₄ Solution Slabs

Values of k_{eff} calculated for the critical infinite slabs of Table V by HRXN-ANISN, by GLASS-ANISN, and by MGBS-TGAN are given in Table X. The order of listing is the same as in Table V. The uncertainty in k_{eff} associated with the experimental uncertainty of ± 0.2 cm in the slab thickness was investigated with HRXN-ANISN (S_{∞}) by increasing the thickness by 0.2 cm. The magnitude of the resulting effect appears in Table X as the parenthetic quantities in the appropriate column. The effect should be about the same with the other methods. The variations in the magnitudes of the difference obtained for bare and reflected slabs by the different methods are surprising. However, the reflected slab results are more directly pertinent to the calculation of limits since reflection is usually assumed. From a comparison of the values of k_{eff} in Table X with those plotted on Figs. 1, 2, and 3, there appears to be

TABLE X

Calculated Values of k_{eff} of the Experimental Critical Infinite Slabs of $\text{Pu}(\text{NO}_3)_4$ Solution Listed in Table V

Plutonium Concentration Hydrogen-to-Fissile Plutonium Atomic Ratio	Reflector	k_{eff}		
		HRXN-ANISN (S_{∞})	GLASS-ANISN (S_{∞})	MGBS-TGAN
446	None	0.9999 (0.0085) ^a	1.0451	1.0230
446	Water	1.0090 (0.0087)	1.0322	1.0242
411	None	0.9998 (0.0078)	1.0429	1.0184
411	Water	0.9948 (0.0081)	1.0256	1.0152
458	None	1.0153 (0.0060)	1.0431	1.0187
458	Water	1.0074 (0.0063)	1.0273	1.0171
179	None	1.0164 (0.0057)	1.0455	1.0224
179	Water	1.0258 (0.0057)	1.0453	1.0290
110.5	None	1.0201 (0.0050)	1.0445	1.0184
110.5	Water	1.0194 (0.0051)	1.0349	1.0160
57.5	Water	1.0265 (0.0043)	1.0346	0.9994
153	None	1.0170 (0.0049)	1.0388	1.0140
153	Water	1.0149 (0.0050)	1.0293	1.0143
102.4	Water	1.0141 (0.0044)	1.0237	1.0058

^aThe quantities in parentheses are the changes in k_{eff} caused by an increase of 0.2 cm in the slab thickness.

no reason to expect the bias from sphere experiments not to be appropriate for slabs. The high concentration of ^{240}Pu in most of the experiments, however, causes deviation from the sphere curves. For HRXN-ANISN, all the points at high ^{240}Pu concentration lie above the curve; hence, the curve is conservative for ^{240}Pu concentrations above those of the curve representing plutonium with $<5\%$ ^{240}Pu . For GLASS-ANISN, points fall on either side of the curve, but tend to fall below it, particularly for reflected systems, at a low hydrogen-to-fissile-plutonium atomic ratio. For MGBS-TGAN, there is a similar trend for the hydrogen-to-fissile-plutonium atomic ratio less than ~ 200 . Adequate allowance must be made for these trends to derive subcritical limits.

IV.C. $\text{Pu}(\text{NO}_3)_4$ Solution Cylinders

Consideration was given with HRXN-ANISN (S_{16})-SPBL and MGBS-TGAN to the P-11 project cylinders of Table II to test the validity of applying bias established for spheres to the calculation of limits for infinite cylinders. Table XI lists values of k_{eff} and axial buckling calculated for the experiments, in the same order as Table II. When comparison is made between the HRXN-ANISN-SPBL results and values at the same H/ ^{239}Pu ratio read from Fig. 1, it is apparent that this method of treating finite bodies overestimates k_{eff} . When the overestimation is plotted against axial buckling, there is considerable scatter, but a

linear relation going to zero at zero axial buckling does not appear unreasonable (a least-squares fit to the data gives $\Delta k_{\text{eff}} = 0.0278$ at $B_z^2 = 0.01 \text{ cm}^{-2}$); hence, Fig. 1 and presumably Fig. 2 should be applicable to infinite cylinders. Deviations of values calculated by MGBS-TGAN from Fig. 3 show little dependence on axial buckling; the average deviation for axial bucklings $<0.006 \text{ cm}^{-2}$ is -0.0015 .

Correlations of HRXN-ANISN (S_{16})-SPBL, GLASS-ANISN (S_{16})-SPBL, and MGBS-TGAN were made with the experiments with high-burnup plutonium. Although the water reflector extended to the top of the vessel, which had a steel cover, the top was assumed bare. To force the mesh assignment scheme in ANISN to treat the bulk of the plutonium solution as an intermediate region, the solution was subdivided into a thin upper layer and the remainder. Differences between extrapolation distances for finite and infinite vessels should have less effect for these large cylinders than for small vessels, and the SPBL treatment should not introduce much, if any, overestimate of k_{eff} . (Axial bucklings ranged from 0.001 to 0.003 cm^{-2} .) The correlations, listed in the same order as in Table VI and recorded in Table XII, seem to bear this out when they are compared with KENO Monte Carlo calculations¹¹ made with the same cross sections. The HRXN-ANISN-SPBL results fall well above the curve in Fig. 1; hence, as concluded from the slab experiments, applying the bias of Fig. 1 to the calculation of subcritical limits by HRXN-ANISN for

TABLE XI
Calculated Values of k_{eff} of the Experimental Critical
Cylinders of $\text{Pu}(\text{NO}_3)_4$ Solution Listed in Table II

Plutonium Concentration $\text{H}/^{239}\text{Pu}$	HRXN-ANISN (S_{16})-SPBL		MGBS-TGAN	
	k_{eff}	B_h^2 (cm^{-2})	k_{eff}	B_h^2 (cm^{-2})
333.3	>0.9748	0.00259	>0.9990	0.00278
234.8	1.0102	0.00524	1.0187	0.00572
261.6	1.0130	0.00506	1.0214	0.00552
303.0	1.0059	0.00473	1.0159	0.00515
352.5	1.0092	0.00417	1.0195	0.00452
422.5	1.0021	0.00349	1.0136	0.00376
479.0	1.0004	0.00297	1.0120	0.00319
333.3	1.0099	0.00675	1.0122	0.00733
335.4	1.0055	0.00693	1.0085	0.00753
414.1	1.0023	0.00613	1.0055	0.00664
526.1	1.0009	0.00478	1.0037	0.00514
663.8	0.9948	0.00334	0.9975	0.00355
408.2	1.0179	0.00782	1.0151	0.00845
529.9	1.0064	0.00666	1.0034	0.00715
553.8	1.0135	0.00630	1.0096	0.00676
603.9	1.0060	0.00482	1.0027	0.00516
663.8	1.0026	0.00519	0.9984	0.00554
659.7	1.0021	0.00318	0.9995	0.00338
774.1	1.0065	0.00366	1.0012	0.00387
843.0	1.0077	0.00279	1.0020	0.00294
234.8	1.0253	0.01073	1.0205	0.01159
536.9	1.0152	0.00819	1.0083	0.00876
616.6	1.0173	0.00699	1.0089	0.00746
719.1	1.0182	0.00596	1.0082	0.00633
841.2	1.0116	0.00475	1.0007	0.00501
983.2	1.0072	0.00308	0.9953	0.00322

high concentrations of ^{240}Pu appears quite conservative. However, applying the bias of Fig. 2 or 3 to the same calculations by GLASS-ANISN or MGBS-TGAN appears slightly nonconservative since the results fall slightly below the curves and adequate allowance for bias and uncertainty must be made.

IV.D. PuO_2 Compacts

Correlations with the critical experiments with PuO_2 compacts described in Table VII are given in Table XIII. The methods used were HRXN-ANISN and GLASS-ANISN. The quadrature in ANISN was S_{16} . (The small difference between S_{16} and S_{∞} in cases studied so far is hardly worth consideration, and certainly is not for the compacts in view of the large error flags.) The critical buckling³¹ derived from the bare cuboid dimensions and a calculated bare extrapolation distance was 0.02620 cm^{-2} . Those calculated by HRXN and GLASS were 0.028825 and 0.028517 cm^{-2} , respectively. Extrapolation to the reflected slab is somewhat uncertain, but the critical height and k_{eff} extrapolation give the best agreement with Monte Carlo results obtained by KENO with the same cross sections. It is worth noting that despite similarities in critical bucklings and migration areas calculated by HRXN and GLASS, k_{eff} values are appreciably different and the difference reverses sign for reflected assemblies compared to bare assemblies.

IV.E. Plutonium Metal

Correlations with the three metal sphere experiments of Table VIII are given in Table XIV. The two bare sphere correlations were made to see how well ^{240}Pu is handled in metal systems. In the GLASS-ANISN calculations, gallium was replaced by nickel

TABLE XII
Calculated Values of k_{eff} of the Experimental Critical Cylinders of $\text{Pu}(\text{NO}_3)_4$ Solution, of High "Burnup," Listed in Table VI

Plutonium Concentration Hydrogen-to-Fissile- Plutonium Atomic Ratio	k_{eff}		
	HRXN-ANISN (S_{16})-SPBL	GLASS-ANISN (S_{16})-SPBL	MGBS-TGAN
301.4	1.0257	1.0195	1.0004
378.4	1.0352	1.0239	1.0036
451.5	1.0295	1.0230	1.0016
535.5	1.0288	1.0214	0.9992
614.2	1.0285	1.0202	0.9974
722.5	1.0278	1.0181	0.9946
845.8	1.0276	1.0163	0.9927
1030	1.0282	1.0141	0.9904
1196	1.0273	1.0110	0.9872

TABLE XIII

Correlation with Critical Experiments with PuO₂ Compacts

Reflected Cuboids			
Height (cm)	k_{eff}		
	HRXN-ANISN-SPBL	GLASS-ANISN-SPBL	
10.03	1.1256	1.1151	
8.98	1.1201	1.1118	
7.97	1.1107	1.1053	
6.86	1.0970	1.0960	
5.95	1.0837	1.0874	
Infinite Slabs			
Reflector	Extrapolation Method	k_{eff}	
		HRXN-ANISN	GLASS-ANISN
None Plexiglas	λ^a	1.0485 ± 0.0184	1.0252 ± 0.0182
	λ^b	0.9921 ± 0.0409	1.0212 ± 0.0380
	Critical height ^c	1.0228 ± 0.0093	1.0497 ± 0.0086
	k_{eff}^d	1.0335	1.0536

^aBased on the calculated difference in extrapolation distance for a cube and an infinite slab.

^bExtrapolation of the effective extrapolation distance as a function of the inverse cross-sectional area.

^cExtrapolation of the critical height as a function of the inverse cross-sectional area.

^dLeast-squares linear extrapolation of SPBL k_{eff} as a function of transverse buckling.

because there are no cross sections for gallium in the GLASS libraries.

V. SUBCRITICAL LIMITS

The limits in the ANSI Standard for a Pu(NO₃)₄ solution apply only to uniform aqueous solutions. They take no credit for free nitric acid and hence in practice would generally have a margin of subcriticality additional to that allowed in calculations since to prevent polymerization and precipitation of the plutonium and hence to maintain a uniform solution,

TABLE XIV

Correlation with Plutonium Metal Spheres

Reflector	²⁴⁰ Pu (%)	k_{eff}	
		HRXN-ANISN (S_{∞})	GLASS-ANISN (S_{∞})
None	4.5	1.0018 ± 0.0017	0.9965
None	20.1	1.0082 ± 0.0022	0.9947
Water	5.18	0.9951 ± 0.0012	1.0063

it is necessary to have a nitric acid concentration¹⁹ of ~1.5 M. However, it would be improper to count on this in deriving the limits. The user of the Standard has the right to expect that the limiting values would really be subcritical under the stated conditions. The limits were calculated for units surrounded by an effectively infinite, contiguous water reflector with no intervening vessel wall and are applicable to any other reflection or interaction condition having no greater effect on k_{eff} .

All three methods, HRXN-ANISN, GLASS-ANISN, and MGBS-TGAN, were used for the recalculation of limits for Pu(NO₃)₄ solutions. The S_n quadrature was S_{16} , the small difference between S_{∞} and S_{16} being ignored. The MGBS-TGAN calculation was used partly because of its extended use in the past, including generation of limits for the mixed-oxide Standard.³⁵

Minimum critical parameters calculated by the three methods for water-reflected aqueous solutions of Pu(NO₃)₄ at 20°C with 100% ²³⁹Pu, as in the Standard, are given in Table XV. The minima were determined graphically from plots of each parameter as a function of concentration. The parameters are calculated to correspond to critical values of k_{eff} , read from Figs. 1, 2, and 3. The MGBS-TGAN results for mass, cylinder diameter, and slab thickness are approximately equal to the subcritical limits in the Standard.¹ Included in Table XV are results obtained by Richey,²¹ whose calculations served as the basis for limits in the Standard. His method was 18-group diffusion theory, with thermal group constants averaged over a Wigner-Wilkins spectrum and epithermal group constants derived from a 64-group B_1 calculation, and agreed well with experiments, with essentially no bias. The disagreement among methods all normalized to the same critical experiments data is somewhat surprising, particularly in the case of mass, since many experiments were performed in the concentration range where minimum mass occurs. The spread in values corresponds to ~2% in k_{eff} .

A careful study of each method would be necessary to discover the sources of the discrepancies. There may be trends in the bias as a function of nitrate and ²⁴⁰Pu concentration that are not readily apparent. Richey's use of a density formula in his parametric survey calculations as opposed to his use of analytical data in correlating with experiments may have introduced some error. The treatment of the stainless steel vessel wall may introduce some error. Back calculation of two reflected sphere experiments with the critical values of k_{eff} determined in correlations were made with and without the steel

³⁵"American National Standard for Nuclear Criticality Control and Safety of Homogeneous Plutonium-Uranium Fuel Mixtures Outside Reactors," ANS-8.12-1978, American Nuclear Society (1978).

TABLE XV

Minimum Critical Parameters of Aqueous Solutions of $\text{Pu}(\text{NO}_3)_4$ with 100% ^{239}Pu

Parameter	HRXN-ANISN	GLASS-ANISN	MGBS-TGAN	Richey
Plutonium mass (kg)	0.536	0.526	0.510	0.547
Cylinder diameter (cm)	16.12	15.96	15.74	16.30
Slab thickness (cm)	5.94	6.02	5.76	6.21
Volume (ℓ)	8.22	7.89	7.81	8.32
Concentration (g Pu/ℓ)	7.62	7.58	7.46	
Hydrogen-to-plutonium atomic ratio	3475	3490	3546	
Areal density (g Pu/cm ²)	0.268	0.272	0.262	

walls. With the walls present, experimental conditions were reproduced satisfactorily, demonstrating the correctness of the radius search corresponding to a specified value of k_{eff} . Without the walls, MGBS-TGAN gave the lowest masses, indicating it calculates the greatest effect; HRXN-ANISN was next. Differences were small, however, slightly less than 1% in mass between GLASS-ANISN and MGBS-TGAN.

Calculations were extended to the minimum critical mass of water-reflected uniform, homogeneous $\text{PuO}_2\text{-H}_2\text{O}$ mixtures. The HRXN-ANISN, GLASS-ANISN, and MGBS-TGAN calculations yielded, respectively, 525, 512, and 496 g Pu. Richey's value was 531 g. At the low concentration at which the minimum mass occurs, it makes little difference whether the mixture is $\text{Pu-H}_2\text{O}$, $\text{Pu}_2\text{O}_3\text{-H}_2\text{O}$, or a fictitious $\text{PuO}_2\text{F}_2\text{-H}_2\text{O}$ for which other calculations have been made. A semi-empirical analysis of the P-11 project data led³⁶ to a minimum critical mass of 506 g. An analysis of the data with an earlier version of MGBS-TGAN (Ref. 37) having a slightly different resonance treatment⁶ and with an empirical correction made for the vessel walls resulted in very little bias. Calculated bucklings, after allowance for slight changes in cross sections to conform to those used in the data analysis but without allowance for bias, led to a minimum critical mass of 498 g Pu. Subsequent use of this analysis with the bias expressed as a function of concentration led³⁸ to a minimum critical mass of 512 g. In a compendium of critical mass data,³⁹ the minimum of the mass versus concentration curve is ~ 510 g. The experimenters in the P-11 project concluded that the minimum critical mass was

509 g contained in the thin steel shell of the experiments.²³ Without the shell, the mass would be reduced to ~ 490 g.

It was thought that perhaps part of the reason for the discrepancy in the results obtained by the three methods of calculation might lie in differences in the "eyeball" fits to the data in Figs. 1, 2, and 3. Accordingly, the critical mass calculations for $\text{Pu}(\text{NO}_3)_4$ and PuO_2 were normalized to the experiment with plutonium containing 0.54% ^{240}Pu at 27.39 g Pu/ℓ. For 0.12 M Pu [$\text{H}/\text{Pu} = 915.2$ for $\text{Pu}(\text{NO}_3)_4$, 920.9 for PuO_2], the critical masses calculated by HRXN-ANISN, GLASS-ANISN, and MGBS-TGAN normalized to the curves in Figs. 1, 2, and 3 were, respectively, 539, 529, and 515 g Pu for $\text{Pu}(\text{NO}_3)_4$ and 528, 517, and 501 g Pu for PuO_2 . Normalized to the single experiment, the results were 532, 525, and 517 g Pu, and 522, 513, and 503 g Pu, respectively. Thus, the normalization is partly responsible for the discrepancy.

The selection of limits is necessarily somewhat arbitrary. Those presently in the Standard for mass, cylinder diameter, slab thickness, and volume of $\text{Pu}(\text{NO}_3)_4$ solutions are purportedly values calculated by Richey²¹ to correspond to a k_{eff} of 0.98. However, the mass and volume limits in the Standard are slightly higher and were taken from an earlier paper.⁴⁰ From an examination of the scatter about the curves of Figs. 1, 2, and 3 and from the experimental uncertainties expressed in terms of variations in k_{eff} , it would appear that a margin in k_{eff} of 0.01 should be sufficient to assure subcriticality, i.e., that conditions corresponding to $k_{\text{eff}} = (1 + \text{bias} - 0.01)$ should be subcritical. The conditions for which the limits are given represent some extension of experimental conditions to 0% ^{240}Pu , zero nitric acid molarity, and zero vessel wall thickness, but there are no obvious variations in the bias with these parameters. For good measure, however, it is desirable to assign an extra margin (0.01), making the total margin 0.02, but with three (four including Richey's) methods, a margin

³⁶H. K. CLARK, "Handbook of Nuclear Safety," DP-532, Savannah River Laboratory (1961).

³⁷H. K. CLARK, "Bucklings of Pu-H₂O Systems," DP-701, Savannah River Laboratory (1962).

³⁸H. K. CLARK, *Nucl. Sci. Eng.*, **24**, 133 (1966).

³⁹H. C. PAXTON, J. T. THOMAS, D. CALLIHAN, and E. B. JOHNSON, "Critical Dimensions of Systems Containing U²³⁵, Pu²³⁹, and U²³³," TID-7028, Technical Information Center (1964).

⁴⁰C. R. RICHEY, *Trans. Am. Nucl. Soc.*, **9**, 515 (1966).

this great applied to the most conservative, particularly when it may have the most approximations, appears excessive. On the other hand, unless a method can clearly be rejected, results calculated by a second method with margin 0.02, which the first method predicts would be critical, should not be accepted as limits. Thus, the limits in the Standard that were predicted by MGBS-TGAN to be critical are too large, even though Richey's method looks quite good.

Table XVI lists "limits" (i.e., parameters corresponding to a margin in k_{eff} of 0.02) calculated by the four methods together with limits now in the Standard and limits proposed for the revised Standard. It is worth pointing out that the margin in k_{eff} is not on the same basis for the two ANISN methods as for MGBS-TGAN. In the former methods, k_{eff} is number of neutrons produced per fission source neutron for a steady-state solution. In TGAN, a fictitious transverse buckling increment is added to each region such that the core buckling results in the desired k_{eff} calculated as $k/(1 + M^2B^2)$. It is apparent by comparing Tables XV and XVI that a margin of 0.02 in k_{eff} produces a larger change in a parameter in TGAN than in ANISN. The proposed limits are generally subcritical by a margin of ~ 0.01 relative to MGBS-TGAN critical values. The concentration limit in the Standard was reduced in the 1975 revision from its original value as the result of doubts,⁴¹ based on data then available, that it was subcritical and as the result

of a reexamination of experimental data.⁴² The recent experiments in the large sphere²⁵ permit it to be raised to its former value. The slurry mass limit has been left at its former value although the margin of subcriticality may be smaller than that supposed.³⁸

In Tables XVII, XVIII, and XIX, "limits" (again parameters corresponding to a margin of 0.02 relative to the curves of Figs. 1, 2, and 3) are calculated for $\text{Pu}(\text{NO}_3)_4$ solution in which the plutonium contains 5% ^{240}Pu and 0.5% ^{241}Pu , 15% ^{240}Pu and 6% ^{241}Pu , and 25% ^{240}Pu and 15% ^{241}Pu by weight. In plutonium actually encountered, ^{238}Pu and ^{242}Pu are present. However, it is conservative to either treat them as ^{239}Pu or omit them from the composition in computing the percentage of ^{240}Pu and ^{241}Pu . Also given in the three tables are suggested limits for the revised Standard. The latter two compositions are those adopted for the mixed-oxide Standard.^{34,35} The other composition was an intermediate one that seemed to offer some utility. The ^{241}Pu concentration was selected on the basis of compositions in the experiments with which correlations were made. Increasing it to 1.5% ^{241}Pu reduces the margin of subcriticality by only ~ 0.002 , as calculated by MGBS-TGAN, a fairly insignificant amount; hence, the suggested limits should be valid up to $\sim 1.0\%$ ^{241}Pu .

The curves in Figs. 1, 2, and 3 are appropriate for the 5% ^{240}Pu composition; many of the experiments were with plutonium containing 4.6% ^{240}Pu . As

⁴¹H. K. CLARK, *Trans. Am. Nucl. Soc.*, 17, 278 (1973).

⁴²C. R. RICHEY, *Nucl. Sci. Eng.*, 55, 244 (1974).

TABLE XVI

Limits for Aqueous Systems Containing Plutonium 100% ^{239}Pu

Parameter	Solutions of $\text{Pu}(\text{NO}_3)_4$					
	Standard	Source	HRXN-ANISN	GLASS-ANISN	MGBS-TGAN	Proposed
Plutonium mass (kg)	0.51	0.499 ^a	0.489	0.477	0.453	0.480
Cylinder diameter (cm)	15.7	15.68 ^a	15.58	15.42	15.02	15.4
Slab thickness (cm)	5.8	5.79 ^a	5.62	5.68	5.27	5.5
Volume (ℓ)	7.7	7.53 ^a	7.55	7.24	6.97	7.3
Concentration (g Pu/ℓ)	7.0	7.0 ^b	7.35	7.29	7.16	7.3
Hydrogen-to-plutonium atomic ratio	---	---	3600	3630	3700	3630
Areal density (g Pu/cm ²)	0.25	0.25 ^c	0.255	0.254	0.245	0.25
	PuO ₂ -H ₂ O Slurry					
Plutonium mass (kg) (uniform slurry)	---	$\sim 0.470^c$	0.478	0.466	0.444	---
Plutonium mass (kg) (nonuniform slurry)	0.450	0.450 ^c	---	---	---	0.450

^aReference 21.

^bReferences 41 and 42.

^cReference 38.

TABLE XVII

Limits for Aqueous Solutions of $\text{Pu}(\text{NO}_3)_4$ with $\geq 5\%$ ^{240}Pu , $\leq 0.5\%$ ^{241}Pu

Parameter	HRXN-ANISN	GLASS-ANISN	MGBS-TGAN	Proposed
Plutonium mass (kg)	0.580	0.576	0.549	0.570
Cylinder diameter (cm)	17.38	17.53	17.19	17.4
Slab thickness (cm)	6.72	7.01	6.59	6.7
Volume (ℓ)	10.03	10.07	9.88	10.0
Concentration (g Pu/ℓ)	7.89	7.84	7.70	7.8
Hydrogen-to-plutonium atomic ratio	3350	3373	3435	3400
Areal density (g Pu/cm ²)	0.282	0.283	0.272	0.28

TABLE XVIII

Limits for Aqueous Solutions of $\text{Pu}(\text{NO}_3)_4$ with $\geq 15\%$ ^{240}Pu , $\leq 6\%$ ^{241}Pu

Parameter	HRXN-ANISN	GLASS-ANISN	MGBS-TGAN	Proposed
Plutonium mass (kg)	0.778	0.806	0.764	0.78
Cylinder diameter (cm)	19.48	20.02	19.62	19.5
Slab thickness (cm)	8.02	8.55	8.05	8.0
Volume (ℓ)	13.55	14.36	13.94	13.6
Concentration (g Pu/ℓ)	9.00	9.01	8.80	8.9
Hydrogen-to-plutonium atomic ratio	2937	2935	3005	2980
Areal density (g Pu/cm ²)	0.338	0.343	0.331	0.34

TABLE XIX

Limits for Aqueous Solutions of $\text{Pu}(\text{NO}_3)_4$ with $\geq 25\%$ ^{240}Pu , $\leq 15\%$ ^{241}Pu

Parameter	HRXN-ANISN	GLASS-ANISN	MGBS-TGAN	Proposed
Plutonium mass (kg)	1.023	1.109	1.027	1.02
Cylinder diameter (cm)	21.25	22.25	21.51	21.3
Slab thickness (cm)	9.11	9.91	9.24	9.2
Volume (ℓ)	17.21	19.10	17.86	17.2
Concentration (g Pu/ℓ)	10.23	10.34	10.02	10.2
Hydrogen-to-plutonium atomic ratio	2587	2558	2640	2600
Areal density (g Pu/cm ²)	0.402	0.416	0.396	0.40

pointed out earlier, the curve in Fig. 1 appears conservative for plutonium containing 18 to 43% ^{240}Pu as judged from the slab and large cylinder experiments. The curve in Fig. 2 may be slightly nonconservative. The curve in Fig. 3 appears appropriate for the higher ^{240}Pu concentration at hydrogen-to-fissile-plutonium atomic ratios >200 . The range of the hydrogen-to-fissile-plutonium atomic ratio within which the critical concentration, mass, and dimensional minima occur shrinks at both ends with increasing ^{240}Pu concentration from 60 to 3500 at 0% ^{240}Pu to 200 to

2500 at 25% ^{240}Pu ; hence, the curve in Fig. 3 should not introduce appreciable nonconservatism into MGBS-TGAN calculations. The largest difference in limits occurs for 25% ^{240}Pu and is in the expected direction. A margin from the curve of Fig. 2 greater than 0.03 (rather than 0.02 as used in the calculation) would be required to bring the GLASS-ANISN results in line with the others.

Only MGBS-TGAN calculations were used to derive mass limits for PuO_2 slurries with ^{240}Pu concentrations $>5\%$. In view of the lack of any indication of

nonconservatism in MGBS-TGAN and of the small increase in k_{eff} (~ 0.007) resulting³⁸ from distributing the minimum critical mass in a uniform distribution optimally, it was concluded that masses calculated by MGBS-TGAN for uniform distributions with Δk_{eff} of 0.02 relative to the curve of Fig. 3 would be subcritical for any nonuniform distribution. Masses of plutonium calculated in this manner for 5, 15, and 25% ²⁴⁰Pu combined, respectively, with 1.5, 6, and 15% ²⁴¹Pu are 530, 740, and 990 g.

Besides the limits for aqueous systems, the Standard¹ contains limits for plutonium metal surrounded by no better reflector than water. These limits were calculated by Roach and Smith⁴³ prior to the critical experiment with the water-reflected metal sphere.³³ As indicated previously, it is desirable to recalculate them and to extend them to oxide. The two methods adopted for the calculations were HRXN-ANISN and GLASS-ANISN. For metal, the quadrature was extrapolated to S_{∞} , but for oxide, S_{16} was adopted. As is apparent from Table XIII, the bias for the oxide calculation has a large element of uncertainty. However, it appears that adopting the bias for a water-reflected sphere (Table XIV) for both metal and oxide calculations should certainly be conservative for oxide. As in the solution calculations, a margin of 0.02 was allowed to assure subcriticality.

Plutonium metal was assumed to have a density of 19.82 (Lange's Handbook) and oxide a density of 11.46 g/cm³. The calculations were made for 100% ²³⁹Pu, but apply to any isotopic composition (which may include ²³⁸Pu), provided ²⁴⁰Pu exceeds ²⁴¹Pu

(calculations for 50-50 ²⁴⁰Pu-²⁴¹Pu gave a much higher critical mass than for ²³⁹Pu). Although ²³⁸Pu may have a lower bare critical mass than ²³⁹Pu, such is not the case with water reflection. Calculations were made both for dry oxide and damp oxide (H/Pu = 0.45, 1.48% H₂O) as for the mixed-oxide Standard,^{34,35} but limits were lower for dry oxide. However, as the hydrogen-to-plutonium atomic ratio increases, the mass must eventually drop; hence, some limit on the ratio is necessary and it might as well be that adopted for the mixed-oxide Standard. In the damp oxide, volumes of water and oxide were assumed additive. The limits are not valid if the volume of damp oxide is less than the sum of the volume of oxide at 11.46 g/cm³ plus that of water at 1 g/cm³. Half-density oxide is simply damp oxide with 50% voids. The calculated limits are given in Table XX. For metal, the agreement of the two methods with each other and with the limits presently in the Standard is excellent.

VI. CAUTIONARY REMARKS

A note of caution needs to be introduced regarding the mass limits for metal and oxide and the volume limits for solutions. These were calculated for spheres, but it has been suggested^{44,45} that for water-reflected, undermoderated cores (such as metal, oxide, or even highly concentrated aqueous solutions), a cube or perhaps a cylinder with a height-to-diameter ratio of approximately unity may have a lower

⁴³W. H. ROACH and D. R. SMITH, "Estimates of Maximum Subcritical Dimensions of Single Fissile Metal Units," ORNL-CDC-3, Oak Ridge National Laboratory (1967).

⁴⁴W. R. STRATTON, "Criticality of Single Homogeneous Units," LA-3612, Los Alamos National Laboratory (1967).

⁴⁵E. D. CLAYTON, *Nucl. Technol.*, **23**, 14 (1974).

TABLE XX
Limits for Plutonium Metal and Oxide

Material	Parameter	HRXN-ANISN	GLASS-ANISN	Standard ^a	Proposed
Metal	Mass plutonium (kg)	5.05	5.03	4.9	5.0
	Cylinder diameter (cm)	4.39	4.38	4.4	4.4
	Slab thickness (cm)	0.70	0.63	0.65	0.65
Oxide	Mass plutonium (kg)	11.06	10.17	---	10.2
	Mass PuO ₂ (kg)	12.54	11.53	---	11.5
	Cylinder diameter (cm)	7.47	7.22	---	7.2
	Slab thickness (cm)	1.60	1.41	---	1.4
Half-density oxide	Mass plutonium (kg)	29.93	27.00	---	27.0
	Mass PuO ₂ (kg)	33.94	30.62	---	30.6
	Cylinder diameter (cm)	13.10	12.56	---	12.6
	Slab thickness (cm)	3.20	2.82	---	2.8

^aReference 1.

critical volume than a sphere. A critical mass of methylmethacrylate (Plexiglas)-reflected PuO_2 that is 14% lower for a cube than for a sphere has been reported, but the result was not considered definitive because of experimental uncertainties.³¹ However, it seems more appropriate to ascribe the lack of definitude to uncertainties in the conversion, apparently by one-dimensional transport theory, of experimentally determined critical thicknesses of slabs, with transverse dimensions varying from ~ 2.5 to 6.9 times the thickness to critical sizes of a sphere and of a cube. No details are given as to how the extrapolation distances used in the conversion were calculated; however, an extrapolation distance for the cube (8.13 cm) nearly as large as that for the sphere (8.17 cm) seems questionable.

Experiments⁴⁶ performed with spheres and cylinders of highly enriched uranium metal reflected by water, paraffin, and graphite indicate, respectively, a 2.4% higher, 0.8% lower, and 2.2% higher minimum critical mass for the cylinder than for the sphere. [Intermediate height (H) and diameter (D) values were obtained by Lagrange interpolation of $1/H$ as a function of $1/D$.] The minimum masses occur, respectively, at $H/D = 1.11$, 0.76, and 0.81. In addition, a critical mass of a water-reflected cube of highly enriched uranium $<1\%$ greater than that of a sphere of the same enrichment and density has been reported.⁴⁷

Calculations, done with the two-dimensional transport theory code DDK and Hansen-Roach cross sections, that have been reported⁴⁴ for a water-reflected uranium metal-water mixture ($H/^{235}\text{U} \cong 30$) indicate a minimum critical volume for a cylinder $\sim 2.5\%$ less than that for a sphere, occurring at $H/D \cong 0.82$. On the other hand, calculations made in connection with the present work, with two-group cross

sections and isotropic scattering, nominally for aqueous solution containing 400 g $^{233}\text{U}/\ell$ as UO_2F_2 ($H/U = 61$), gave a minimum critical volume ($\sim 2.6 \ell$) for a water-reflected cylinder 0.9% larger than that of a sphere, at $H/D = 0.87$. The cylinder calculations were made by the TWOTRAN code⁴⁸ with S_{16} quadrature, and the sphere calculations were made by ANISN (Ref. 12), also with S_{16} . (Although results for infinite cylinders obtained by the two methods have been observed to differ by as much as 1% in k_{eff} with S_4 quadrature, agreement is much better with S_{16} . In the present case, ANISN computed $k_{\text{eff}} = 0.9995$ for the infinite cylinder determined by TWOTRAN.) Calculations were also done by ANISN of the diameter of a cylinder at k_{eff} corresponding to two-thirds the critical buckling (to attempt to simulate a cube), and by TWOTRAN of the dimensions of an infinitely long cuboid with a square cross section at the same k_{eff} . The cross-sectional area of the cuboid was 0.1% less than that of the cylinder.

It is difficult to generalize from these few experiments and calculations. The margin in k_{eff} in the limits, however, appears to be sufficient to allow for the possibility that other convex shapes may have a slightly lower critical volume than a sphere. Certainly, this should be the case for metal where, solely for a sphere, an increase of 6% in the limit to 5.3 kg (compared to a critical mass of 5.42 kg), corresponding to a reduction in the margin in k_{eff} to ~ 0.0065 , could be justified due to the precision of the experiment and the small extrapolation to pure ^{239}Pu .

ACKNOWLEDGMENT

This paper was prepared in connection with work performed at the Savannah River Laboratory under contract with the U.S. Department of Energy.

⁴⁶E. C. MALLORY, "Oralloy Cylindrical Shape Factor and Critical Mass Measurements in Graphite, Paraffin, and Water Tamper," LA-1305, Los Alamos National Laboratory (1951).

⁴⁷J. C. HOOGERP, "Critical Masses of Oralloy Lattices Immersed in H_2O ," LA-2026, Los Alamos National Laboratory (1957).

⁴⁸K. D. LATHROP and F. W. BRINKLEY, "TWOTRAN-II: An Interfaced, Exportable Version of the TWOTRAN Code for Two-Dimensional Transport," LA-4848-MS, Los Alamos National Laboratory (1973).